JOURNAL OF CATALYSIS **161,** 310–318 (1996)
ARTICLE NO. 0189

Promoted Pt Catalysts for Automotive Pollution Control: Characterization of Pt/SiO_2, $Pt/CoO_x/SiO_2$, and $Pt/MnO_x/SiO_2$ Catalysts

Y. J. Mergler, A. van Aalst, J. van Delft, and B. E. Nieuwenhuys[1]

Leiden Institute of Chemistry, Gorlaeus Laboratories, Leiden University, P.O. Box 9502, 2300 RA Leiden, The Netherlands

Received August 4, 1995; revised November 27, 1995; accepted January 31, 1996

The characterization of Pt/SiO_2, $Pt/CoO_x/SiO_2$, $Pt/MnO_x/SiO_2$, CoO_x/SiO_2, and MnO_x/SiO_2 catalysts with 5 wt% Pt, 25 wt% MnO_2, 50 wt% Co_3O_4, and 3 wt% Co_3O_4 is described. The $Pt/CoO_x/SiO_2$ catalyst is particularly active in low-temperature CO oxidation, while the $Pt/MnO_x/SiO_2$ catalyst is more active in NO reduction by CO than the unpromoted Pt catalyst. The characterization techniques used are (1) X-ray diffraction, to determine the average particle size and possible alloy formation; (2) CO chemisorption, to determine the specific Pt surface area; and (3) Fourier transform infrared spectroscopy, to study the adsorption of CO and NO and the interaction between CO and NO. The influence of a reductive or oxidative pretreatment is also examined. After a reductive pretreatment the high-loaded $Pt/50CoO_x/SiO_2$ catalyst shows the formation of a PtCo alloy and Co^0 metal. No alloy formation was detected for the $Pt/3CoO_x/SiO_2$ catalyst. Fourier transform infrared measurements show the characteristic bands of linearly adsorbed CO on Pt at 2070 cm^{-1}, and linear and bent NO on cobalt oxide at 1870 and 1790 cm^{-1}, respectively. For the high-loaded $Pt/50CoO_x/SiO_2$ a shoulder at 2023 cm^{-1} is observed and ascribed to CO linearly bound to cobalt metal. An isocyanate band at 2200 cm^{-1} is found for the $Pt/3CoO_x/SiO_2$, $Pt/50CoO_x/SiO_2$, $Pt/MnO_x/SiO_2$, and MnO_x/SiO_2 catalysts on coadsorption of CO and NO.

INTRODUCTION

Major pollutants originating from automotive exhaust gases are CO, hydrocarbons, and NO_x. By using a three-way catalyst (TWC), these components can be removed from the exhaust gases to a large extent. The current TWC consists of the noble metals Pt, (Pd), and Rh (1–3). New legislation in the European Union and the United States mandates that the future automotive exhaust gas emission must fall substantially from current levels. The combination of tougher standards and the increasing number of cars equipped with automotive catalysts may cause a rising demand and concomitant high price for Rh. Thus, it is very relevant to perform research with the objective of finding a replacement for Rh in automotive catalysis. A research program was initiated in which the main objective was to investigate Pt-based, Rh-free catalysts. In this context, several metal oxides were added to a Pt/SiO_2 catalyst and their effects on CO oxidation and NO reduction reactions were studied. For this model study SiO_2 (Aerosil) was chosen as support, since it is relatively inert and, in addition, facilitates interpretation of Fourier transform infrared (FT-IR) and X-ray diffraction (XRD) spectra. It was observed that $Pt/CoO_x/SiO_2$ showed remarkably good low-temperature CO oxidation activity (4–8), while $Pt/MnO_x/SiO_2$ showed good performance in the NO reduction by CO (4, 5, 8). In this paper the preparation and characterization of these selected catalysts are described in more detail.

The main characterization techniques used were determination of the specific Pt surface area by CO chemisorption, estimation of the Pt particle diameter by XRD, and detailed investigation of the metal surfaces by FT-IR of adsorbed CO and NO.

Infrared spectroscopy is one of the techniques that can be used for a more detailed investigation of the geometric and electronic structure of metal surfaces via the adsorption of probe molecules. The chemisorption of CO and NO has often been used to examine the nature of the surface transition metal atoms. The extensive knowledge pertaining to the interaction of these molecules with metal atoms and ions makes their use attractive. It should be noted, however, that the surface complexes formed can be fairly stable and may not necessarily be reaction intermediates. They may also be spectator species (9). In addition, IR spectroscopy is a sensitive tool to study alloy catalysts (10–12). On alloying both the C–O and metal–CO bond strengths may be affected or the second metal may dilute the first metal, thereby reducing the vibrational coupling of the adsorbed molecules on the surface and hence affecting the wavenumber at higher coverages.

In this paper the results obtained on characterization of the catalysts with CO chemisorption and XRD are correlated with the IR results. One purpose was to find out whether the addition of a metal oxide to Pt influences the adsorption of CO and NO and their interaction on Pt. Emphasis is placed on the IR results, and special attention is given to alloy formation and formation of isocyanate.

[1] To whom correspondence should be addressed. Fax: 31-71-5274451.

0021-9517/96 $18.00

EXPERIMENTAL

Catalyst Preparation

To prepare catalysts with the same Pt loading and dispersion, a standard catalyst was made by urea decomposition (13) that contained 5 wt% Pt/SiO_2. The metal oxides were impregnated onto this standard catalyst. This high Pt loading was used to facilitate the FT-IR and XRD experiments and to increase the probability of Pt–CoO_x contacts.

Standard catalyst. The accurate amount of $H_2Pt(OH)_6$ to yield a 5 wt% Pt catalyst was dissolved in hot nitric acid. The Pt solution was added to an acidic silica suspension with a pH of 2. Urea was added and the suspension was stirred and heated to about 80°C. After 24 or 48 h the suspension was cooled and filtered. The resulting Pt/SiO_2 catalyst was dried overnight at 100°C and reduced in H_2 for 3 h at 400°C.

The standard catalyst was impregnated with the proper amount of a solution of the metal nitrate precursor to yield 3 wt% Co_3O_4 or 25 wt% MnO_2. The relative amounts of Co_3O_4 and MnO_2 are based on earlier studies of CO oxidation over promoted Pt catalysts (4). These studies showed that 5 wt% Pt/SiO_2 with 3 wt% Co_3O_4 or 25 wt% MnO_2 performs well in CO oxidation by O_2 and NO. The impregnated standard catalyst was dried overnight at 100°C and reduced or oxidized prior to the infrared measurements.

To compare the Pt/SiO_2, $Pt/CoO_x/SiO_2$, and $Pt/MnO_x/SiO_2$ properly, 3 wt% CoO_x/SiO_2 and 25 wt% MnO_x/SiO_2 catalysts were also made by impregnation of the silica.

Supported cobalt oxide. By means of homogeneous deposition precipitation (14), 50 wt% Co_3O_4/SiO_2 was made. The catalyst was filtered and dried overnight at 100°C. The cobalt catalyst was oxidized in air for 3 h at 400°C. Pt was impregnated onto this catalyst, resulting in 5 wt% $Pt/50CoO_x/SiO_2$.

Nomenclature. Throughout this paper a standard nomenclature has been adopted to designate the catalyst weight percentages. The Pt loading was always 5 wt%. Pt/SiO_2 is the standard catalyst with 5 wt% Pt, $Pt/CoO_x/SiO_2$ is the standard catalyst impregnated with 3 wt% Co_3O_4, $Pt/MnO_x/SiO_2$ is the standard catalyst impregnated with 25 wt% MnO_2. The catalysts with higher loadings of cobalt were prepared by homogeneous deposition precipitation, in which the cobalt was deposited first, and have the nomenclature $50CoO_x/SiO_2$ and $Pt/50CoO_x/SiO_2$.

Pretreatment. Prior to XRD or FT-IR measurements the catalysts were reduced in flowing H_2 for 3 h at 400°C or oxidized in air for 3 h at 400°C.

Characterization Methods

X-Ray diffraction. XRD measurements were carried out using a Philips Goniometer PW 1050/25 equipped with a Cu 2103/00 X-ray tube. The source provided Cu$K\alpha$ radiation with a wavelength of 1.5418 Å.

CO chemisorption measurements. The adsorption of CO was measured using a Quantasorb Adsorption Apparatus (Quantachrome). After an *in situ* reduction of the catalyst powder at 400°C for 3 h, the catalyst was cooled to room temperature in the H_2 flow. Discrete amounts of CO (0.1 ml) were injected repeatedly until no further CO adsorption could be detected. H_2 (dihydrogen) was used as carrier gas. The dispersion is defined as the number of adsorbed species (e.g., CO) divided by the total number of Pt atoms.

Fourier transform infrared spectroscopy. The infrared spectra were obtained using a single-beam, Mattson Galaxy 2020 Fourier transform infrared spectrometer. The resolution was 4 cm^{-1}, and 32 scans were taken for each spectrum.

Background spectra of the self-supporting disks of the catalysts were taken at 10^{-5} mbar at several temperatures. After addition of 5 mbar CO, 5 mbar NO, or 5 mbar CO + 5 mbar NO, sample spectra were taken at the same temperatures as the background spectra. Subtraction of the background spectra from the sample spectra yielded the absorption spectra. For clarity, the results of the three types of experiments mentioned above are displayed in one or two figures. One should be aware of the fact that slight changes in experimental conditions may cause slight changes in the intensity of the bands.

Since the sample compartment of the spectrometer in which the IR cell was placed was not purged with inert gas, bands of CO_2 and H_2O can appear in the spectra as negative or positive peaks because the concentrations of CO_2 and H_2O in the sample compartment can vary during the measurements. This means that the reaction product CO_2 in CO/NO reactions cannot be distinguished from background CO_2.

The gases used were purchased from Messer Griesheim. CO (99.97%), H_2 (99.999%), O_2 (99.998%), and NO (99.5%) were all used without purification. The disks were reduced *in situ* in 100 mbar H_2 for 1 h at 300°C prior to the actual IR measurements. In some cases an *in situ* oxidative pretreatment was carried out with 100 mbar O_2 for 1 h at 300°C.

RESULTS AND DISCUSSION

CO Chemisorption and X-Ray Diffraction

Table 1 shows the main characteristics of the catalysts obtained by X-ray diffraction and CO chemisorption. The mean particle size was measured by XRD and the Pt dispersion by means of CO chemisorption. It was assumed that one CO molecule adsorbs per surface Pt atom. The Pt dispersion of $Pt/CoO_x/SiO_2$ was not corrected for the CO adsorbed on cobalt. It should be noted that two standard

TABLE 1

Characteristics of the Catalysts

Catalyst	Pt (wt%)	MO (wt%)	Atomic ratio Pt : M	Dispersion (%)	XRD	
					After oxidation	After reduction
Pt/SiO_2	5	—	—	18	—[a]	Pt 160 Å
Pt/SiO_2 (2)[b]	5	—	—	10	—[a]	Pt 60 Å
CoO_x/SiO_2	—	3	—	0	Not measured	Not measured
$50CoO_x/SiO_2$	—	50	—	Not measured	—[a]	—[a]
MnO_x/SiO_2	—	25	—	0	Not measured	Not measured
$Pt/CoO_x/SiO_2$	5	3	1 : 1.5	10[c]	Pt, Co_2O_3	Pt 60 Å
$Pt/MnO_x/SiO_2$	5	25	1 : 15	10	Pt 180 Å, MnO_2 120 Å	Pt 170 Å, MnO 115 Å
$Pt/50CoO_x/SiO_2$	5	50	1 : 8	57[c]	Not measured	CoPt, Co^0

[a] No diffraction peaks were found.
[b] This standard catalyst was used for the cobalt-containing catalysts.
[c] No correction for CO chemisorbed on cobalt.

Pt/SiO_2 catalysts were made. One of them was used for the manganese-containing catalysts and one for the cobalt-containing catalysts. As can be seen in Table 1 these standard catalysts differ in Pt particle size and dispersion. This may be caused by the difference in the duration of the urea decomposition and temperature during the urea decomposition.

The CO-derived dispersion values reveal that the standard Pt/SiO_2 catalyst used for the Co-containing catalysts has a lower dispersion than the standard used for the Mn-containing catalyst (10% versus 18%). However, the XRD results suggest average Pt particle sizes of 60 Å for the Pt catalyst used for the Co-containing catalyst and 160 Å for the standard catalyst used for the preparation of the Mn-containing catalyst. This apparent discrepancy between the dispersion values measured by CO chemisorption and the particle sizes estimated by XRD can be attributed to the fact that XRD is unreliable for measuring true particle size if many small Pt particles are present. The XRD-derived particle size is dominated by the presence of some large metal particles, and the particles smaller than about 30 Å are invisible. Hence, for our discussion the CO-derived values are more reliable than the XRD-derived values. Although the XRD values for the Pt particle diameter are less reliable than the dispersion, the XRD values are included in Table 1 since they provide extra information about possible alloy formation and about the possible coverage of Pt by metal oxides. In the latter case, the Pt particle diameter measured by XRD does not change, whereas the CO-derived dispersion is affected.

Table 1 shows that the XRD-derived particle size of Pt does not change on addition on the metal oxides. The Pt dispersion measured by CO chemisorption, however, decreased on addition of the Mn oxide. Partial covering of the Pt sites by the metal oxide may have occurred. The metal oxides are reduced after treatment in hydrogen at 400°C for 3 h. MnO_2 is reduced to MnO and Co_3O_4 to Co^0. Pure Co_3O_4 is reduced in two steps to Co^0 at 210 and 230°C, while MnO_2 is reduced above 300°C to MnO, according to Glaser (15). Pt may assist the reduction of the metal oxide by hydrogen spillover. At higher Co loading metallic Co and Pt–Co alloy formation were observed after a reductive pretreatment. This catalyst adsorbs large amounts of CO as shown by the high value for the apparent dispersion of the catalyst (Table 1).

Guczi *et al*. studied alumina-supported Pt–Co catalysts with temperature-programmed reduction (TPR) and X-ray photoelectron spectroscopy (XPS) (16, 17). Platinum and cobalt were coimpregnated. For a catalyst with more Pt than Co, the authors suggested that a metallic Pt layer is formed, partly decorating a cobalt surface phase. If more Co than Pt was present, as in our case, metallic Co and a bimetallic PtCo or Pt–Co^0 interface were formed on reduction, besides the metallic Pt and the cobalt surface phase. The cobalt surface phase did not disappear after a mild reduction at 300°C (16).

The spreading of cobalt oxide over a support was studied by Potoczna-Petru and Kepiński (18). They used TEM and electron diffraction to investigate a model Co/SiO_2 catalyst. Calcination at 300 and 400°C led to the formation of Co_3O_4 with an enhanced interaction of the Co phase with SiO_2 which led to spreading. Redispersion of Co_3O_4 particles and their reduction to Co^0 could be obtained by heating the oxidized samples in H_2 at 400°C.

The formation of Pt–Co alloys has been studied in more detail by FT-IR spectroscopy. Since one might expect the segregation of Co to the alloy surface or the breaking up of the alloy particles after on oxidation, the $Pt/50CoO_x/SiO_2$ catalyst was also studied in the presence of O_2.

Fourier Transform Infrared Spectroscopy

As mentioned earlier under Experimental, we cannot ascribe the band at 2360 cm^{-1} unambiguously to CO_2 produced during the reaction between CO and NO. Therefore, no attention is paid to this band. Bands below 1650 cm^{-1}

can be ascribed to nitrate and carbonate-type groups. In our opinion, these bands are not important for the following discussion.

Pt/SiO_2. Figure 1 shows the absorption bands when 5 mbar CO and 5 mbar NO were coadsorbed on the Pt/SiO_2 catalyst. Only one band appeared, at 2070 cm^{-1}, which can be ascribed to CO linearly bound to Pt (19). This band is sharp. No bridge-bonded CO was found and there were no bands indicating NO adsorption. No isocyanate complex bound to Pt was detected at higher temperatures.

$50CoO_x/SiO_2$. Figure 2a shows the adsorption of 5 mbar CO on 50 wt% CoO_x/SiO_2 after a reductive pretreatment. A small band at 2178 cm^{-1} was found, which disappeared after heating above 100°C. Busca *et al.* (20) identified a band at 2180 cm^{-1} when pure, outgassed cobalt oxide was exposed to 100 mbar CO. They ascribed this band to CO bound to Co^{3+} ions. We assign the band at 2178 cm^{-1} to CO bound to Co^{3+}. The adsorption of 5 mbar NO on CoO_x/SiO_2 is shown in Figs. 2b and c. Two characteristic bands for NO bound to cobalt oxide were visible at 1875 and 1788 cm^{-1}. They were assigned to linear and bent NO, respectively (21, 22). Coadsorption of CO and NO led only to bands of linear and bent NO on cobalt oxide, as can be seen in Figs. 2d–f. NO starts to desorb above 200°C. At 300°C all the NO was desorbed. Cooling to room temperature restored the original spectrum (not shown). No indication of NO dissociation was found. This might explain the fact that no isocyanate groups were found.

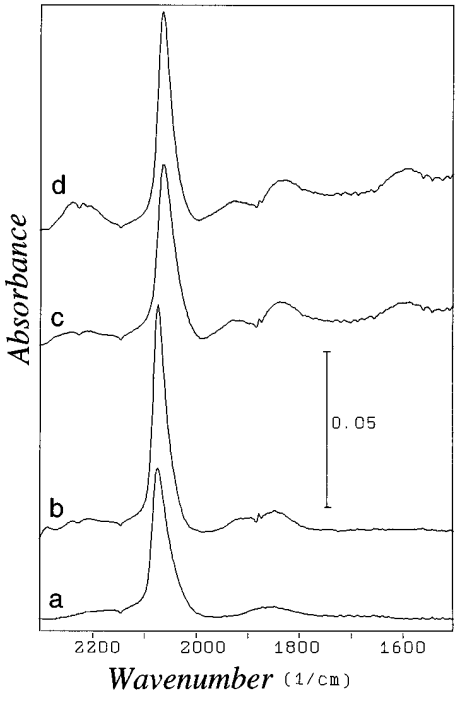

FIG. 1. Infrared spectra of Pt/SiO_2 after a reductive pretreatment. Addition of (a) 5 mbar CO at room temperature and 5 mbar CO + 5 mbar NO at (b) 100°C, (c) 250°C, and (d) 350°C.

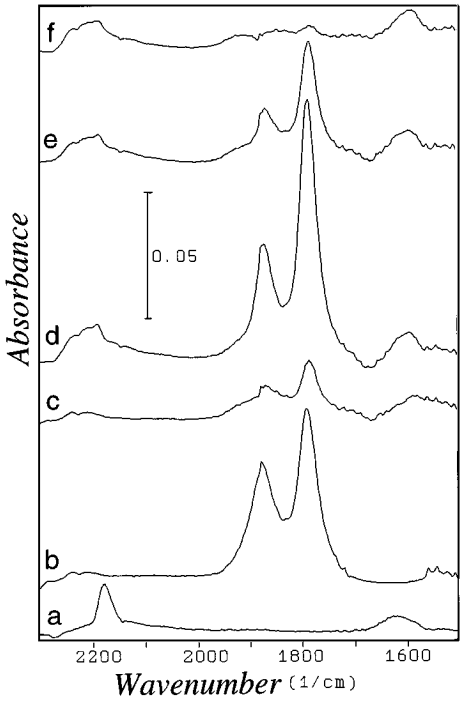

FIG. 2. Infrared spectra of 50 wt% Co_3O_4/SiO_2 after a reductive pretreatment. (a) Addition of 5 mbar CO at room temperature. (b, c) Addition of 5 mbar NO at (b) 100°C and (c) 200°C. (d–f) Addition of 5 mbar CO + 5 mbar NO at (d) 100°C, (e) 200°C, and (f) 300°C.

$Pt/50CoO_x/SiO_2$. Figures 3a–c show the adsorption of 5 mbar CO on $Pt/50CoO_x/SiO_2$ after a reductive pretreatment. A band of CO bound to Co^{n+} is seen around 2170 cm^{-1} at room temperature. A band at 2064 cm^{-1} with a distinct shoulder at 2023 cm^{-1} was also observed. At 300°C the shoulder decreased in intensity. CO linearly bound to Pt shows a band at 2070 cm^{-1} (Fig. 1). On addition of cobalt oxide the band of CO linearly bound to Pt shifted to a lower wavenumber. The shoulder at 2023 cm^{-1} may originate from CO linearly bound to Co^0. Literature values concerning the band position of Co^0–CO are rather diverse. Bands found between 2070 and 2025 were ascribed to CO species linearly bound to Co^0 (23, 24). Gopalakrishnan and Viswanathan (25) described the bands at 1990 and 1800 cm^{-1}, found on CO adsorption on polycrystalline Co surfaces, to linearly and bridged adsorbed CO, respectively. We assume that the shoulder at 2023 cm^{-1} originates from Co^0–CO. This assumption is supported by the CO chemisorption and XRD results (see Table 1). As discussed above, these results show that a large part of the Co of the $Pt50CoO_x/SiO_2$ catalyst is in the metallic state following reduction at 400°C.

Generally, a shift to lower wavenumbers observed on alloying (red shift) is ascribed either to a geometric or to an electronic effect. Several Pt alloys have been investigated

in detail by Toolenaar *et al.* (26, 27). The observed red shifts could be attributed to a simple dilution effect of Pt by the second component (26–28).

Alloying of Pt with Co led to a shift in the position of the CO absorption band to lower wavenumbers. Table 1 shows that for $Pt/50CoO_x/SiO_2$, Co^0 and Co–Pt were detected with XRD after a reduction. The band at 2064 cm^{-1} may well be ascribed to CO linearly bound to Pt, influenced by alloying with cobalt.

Furthermore, Fig. 3 also shows the bands obtained on introduction of 5 mbar NO to the reduced $Pt/50CoO_x/SiO_2$ catalyst (Figs. 3c–h). The characteristic bands of linear and bent NO are found at 1863 and 1791 cm^{-1}. The wavenumber of linearly bound NO has also been shifted toward lower wavenumbers, compared with the NO bands found on $50CoO_x/SiO_2$ (Fig. 2). NO starts to desorb and to dissociate above 200°C (Fig. 3e). A very small band of bent NO was detected at 300°C (Fig. 3g). After cooling to room temperature, the NO absorption bands did reappear with a much lower intensity, which is an indication that part of the NO was dissociated (Fig. 3 h).

Figure 4 shows the $Pt/50CoO_x/SiO_2$ catalyst after a reductive pretreatment when CO and NO are coadsorbed. At 100°C four bands can be distinguished. At 1860 and 1786 cm^{-1} there are the bands of linear and bent NO, at 2062 cm^{-1} there is the band of CO linearly bound to Pt,

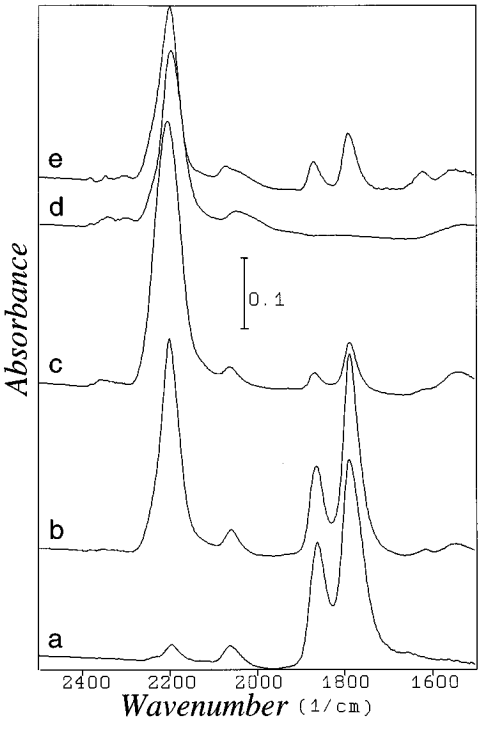

FIG. 4. Infrared spectra of $Pt/50CoO_x/SiO_2$ after a reductive pretreatment. Addition of 5 mbar CO + 5 mbar NO at (a) 100°C, (b) 200°C, (c) 250°C, (d) 350°C, and (e) after cooling to room temperature.

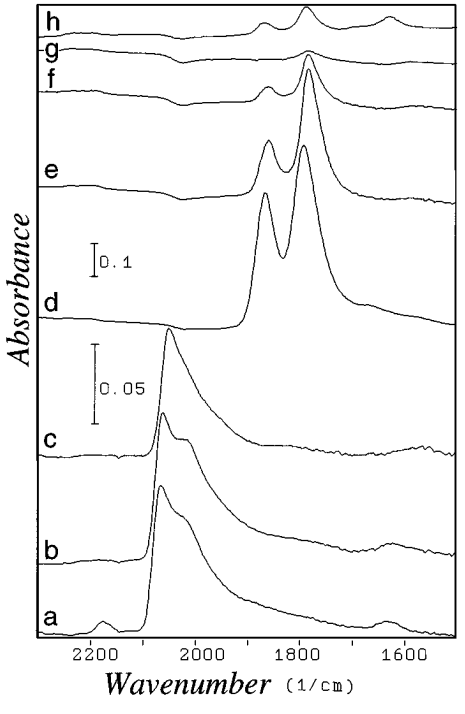

FIG. 3. Infrared spectra of $Pt/50CoO_x/SiO_2$ after a reductive pretreatment. (a–c) Addition of 5 mbar CO at (a) room temperature, (b) 100°C, and (c) 300°C. (d–h) Addition of 5 mbar NO at (d) room temperature, (e) 200°C, (f) 250°C, (g) 300°C, and (h) after cooling to 25°C.

which is a broad band because it also contains a contribution from CO linearly bound to cobalt metal. A new band arose at 2197 cm^{-1}. No band at 2200 cm^{-1} was found on coadsorption of CO and O_2 (see Fig. 5). In addition, the adsorption of CO after oxidation as pretreatment did not lead to the formation of a band at 2200 cm^{-1}. In conclusion, the band at 2200 cm^{-1} cannot be ascribed to CO adsorbed on Co^{3+}. Yao and Shelef (29) found a small band at 2190 cm^{-1} on pure cobalt oxide when CO and NO were coadsorbed, which they ascribed to –NCO on cobalt oxide. We therefore believe that the band at 2197 cm^{-1} originates from isocyanate on cobalt oxide.

With increasing temperature, the isocyanate band grew in intensity. The pressure in the cell dropped, which was an indication of a reaction proceeding between CO and NO. At 350°C (Fig. 4d) the isocyanate band started to decrease in intensity, possibly due to further reaction with NO_a to CO_2 and N_2 (30, 31). Cooling to room temperature restored the original spectrum, although the intensities of the absorption bands were changed, as can be seen in Fig. 4e.

The formation of –NCO can proceed on Pt (19). Migration of the –NCO group to the carrier is possible. This process is rapid or slow, depending on the carrier. Solymosi *et al.* (30) and Anderson and Rochester (32) found that the migration of –NCO to SiO_2 is a very slow process. On alumina, however, this process is so rapid that no isocyanate on Pt could be distinguished (30, 32). We did not find any

–NCO bands on coadsorption of CO and NO at higher temperatures on our Pt/SiO_2 catalyst. This can mean either that 350°C is too low to start the dissociation of NO or that the –NCO reacts further with NO to N_2 and CO_2 (31). The mechanism by which –NCO formation takes place on the $Pt/50CoO_x/SiO_2$ catalyst is not yet clear. Is –NCO formed on Pt with a concomitant migration to cobalt oxide (Model 1)? Alternatively, does CO_a on Pt spill over to N_a on cobalt oxide (Model 2)? Or does the reaction between N_a and CO_a take place only on cobalt oxide (Model 3)? The last model may explain why the –NCO formation starts at temperatures as low as 100°C, while at 100°C NO dissociation on Pt is unlikely due to the inhibition of Pt sites by CO. However, in our opinion, the third model is also rather unlikely since we found no –NCO on coadsorption of CO and NO over our CoO_x/SiO_2 catalyst. Nevertheless, it must be possible to form isocyanate on cobalt oxide, since Yao and Shelef did detect –NCO on their pure cobalt oxide (29). Model 2 is the most likely of the three models. This means that an increase in the intensity of the 2200 cm^{-1} band will be accompanied by a decrease in the intensity of the Pt–CO band.

Figure 5 shows IR spectra for the $Pt/50CoO_x/SiO_2$ catalyst after a reductive pretreatment. In Fig. 5a, 5 mbar CO was adsorbed at 25°C. A broad band at 2060 cm^{-1} attributed to CO on Pt with a shoulder at 2020 cm^{-1} attributed to CO

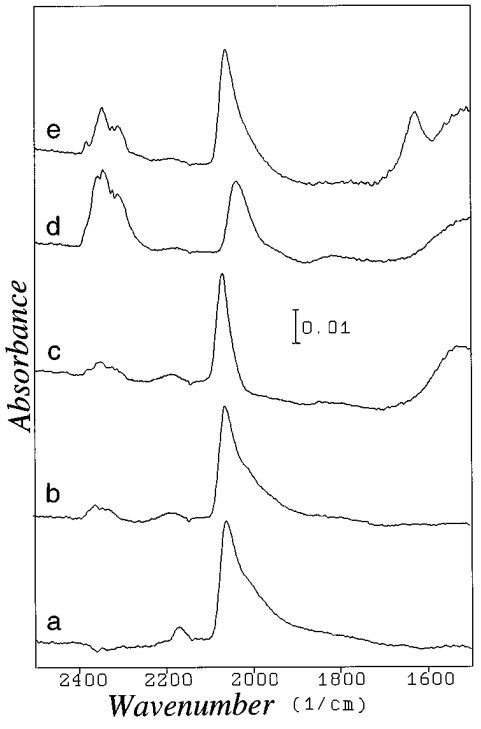

FIG. 5. Infrared spectra of $Pt/50CoO_x/SiO_2$ after a reductive pretreatment. (a, b). Addition of 5 mbar CO at (a) room temperature and (b) 100°C. (c–e) Addition of 5 mbar CO + 2 mbar O_2 at (c) 100°C, (d) 350°C, and (e) after cooling to 25°C.

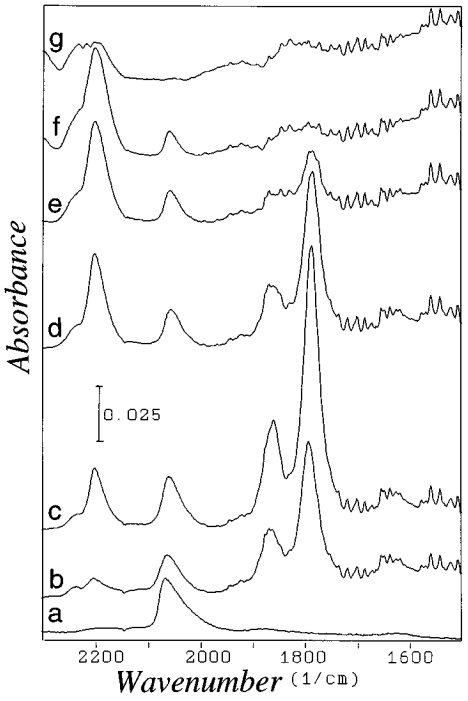

FIG. 6. Infrared spectra: (a) 5 mbar CO introduced to $Pt/CoO_x/SiO_2$ at room temperature. (b–g) Addition of 5 mbar NO and 5 mbar CO at (b) 100°C, (c) 150°C, (d) 200°C, (e) 250°C, (f) 300°C, and (g) 350°C.

on Co^0 is clearly visible. The shoulder disappeared directly on introduction of 2 mbar O_2 at 100°C, as can be seen in Fig. 5c. At this temperature the CO oxidation reaction is fast over $Pt/CoO_x/SiO_2$ (4). At 350°C all the oxygen has reacted with CO to CO_2. Since more CO than O_2 was introduced, CO was left over. Cooling to room temperature should then lead to reappearance of the Pt–CO band. Comparison of Fig. 5a with Fig. 5e shows that this is indeed the case. However, the band has shifted toward higher wavenumbers and the shoulder at 2020 cm^{-1} did not reappear. In fact, this shift had already been observed at 100°C in the presence of CO and O_2 (Fig. 5c). This may indicate that the Co^0 was oxidized and that the alloy particles broke up. Shifts toward higher wavenumbers of CO linearly bound to Pt can also occur when Pt is slightly oxidized (33). Oxidation of Pt at 100°C is, however, very unlikely, especially in a net reducing atmosphere. Therefore, we conclude that O_2 disrupted the alloy particles that were formed on reduction and that O_2 reoxidized Co^0.

$Pt/CoO_x/SiO_2$. Figure 6 shows the adsorption of CO and NO on $Pt/CoO_x/SiO_2$ at different temperatures. First, CO was introduced at room temperature, giving rise to a band at 2066 cm^{-1} of CO linearly bound to Pt. When a $Pt/CoO_x/SiO_2$ catalyst was measured, with 50 wt% CoO_x, following a reduction at 400°C, a band at 2023 cm^{-1} of CO linearly bound to Co^0 was also found (Fig. 3). The band at 2066 cm^{-1} is broader at the base, but no distinct shoulder or

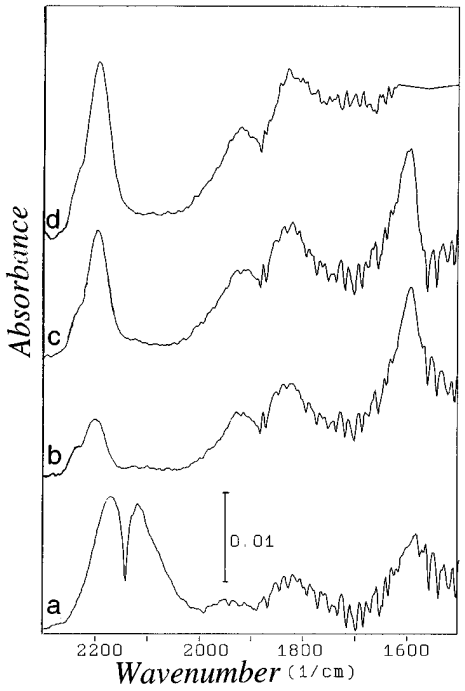

FIG. 7. Infrared spectra of MnO_x/SiO_2 after a reductive pretreatment. Addition of 5 mbar CO + 5 mbar NO at (a) 200°C, (b) 250°C, (c) 300°C, and (d) 350°C.

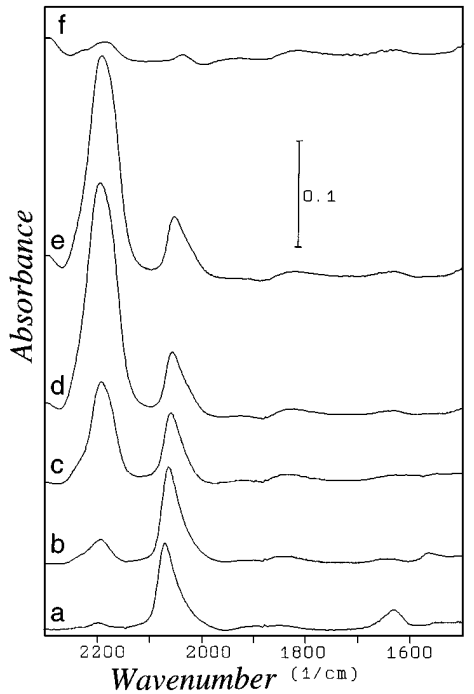

FIG. 8. Infrared spectra of $Pt/MnO_x/SiO_2$ after a reductive pretreatment. Addition of 5 mbar CO and 5 mbar NO at (a) room temperature, (b) 150°C, (c) 300°C, (d) 350°C, $t = 0$ min, (e) 350°C, $t = 17$ min, and (f) 350°C, $t = 46$ min.

band around 2020 cm^{-1} could be distinguished. After the introduction of NO at 100°C, bands of linear and bent NO were found at 1867 and 1792 cm^{-1}, respectively. The band at 2060 cm^{-1} stems from CO linearly bound to Pt. A new band at 2201 cm^{-1} showed up at this temperature, which increased in intensity when the temperature was raised to 250°C.

When the temperature was increased from 200 to 250°C, the bands of linear and bent NO on cobalt oxide almost disappeared, while the intensity of the –NCO band increased. More NO is dissociated at higher temperatures, leading to more N_a and more –NCO. As can be seen in Fig. 6, the increase in intensity of the 2200 cm^{-1} band is accompanied by a decrease in the intensity of the Pt–CO band between 200 and 250°C.

MnO_x/SiO_2. Figure 7 shows the IR spectra observed on coadsorption of CO and NO on the MnO_x/SiO_2 catalyst. No absorption bands of CO or NO were found. Below 250°C the characteristic IR spectrum of CO gas is seen. Isocyanate groups were formed above 250°C when CO and NO were coadsorbed on MnO_x/SiO_2. This means that the dissociation of NO starts around 250°C. Increasing the temperature to 350°C did not decrease the intensity of the isocyanate band as was observed for $Pt/CoO_x/SiO_2$ in Figs. 6f and g.

$Pt/MnO_x/SiO_2$. When NO and CO were added to $Pt/MnO_x/SiO_2$, the formation of –NCO started at around 150°C (see Fig. 8). The isocyanate band grew in intensity when the temperature was raised to 350°C. The bands of Pt–CO and –NCO were not stable at this temperature; they disappeared after 45 min. We detected no bands of linear or bent NO, or CO bands, on manganese oxide.

The area under the isocyanate absorption band was measured. The results are shown in Table 2. The area under an absorption band is related to the amount of adsorbed species. As can be seen in Table 2, more –NCO is formed after a reductive pretreatment and with CO added first.

TABLE 2

Area under the –NCO Bands (A_{-NCO}) for $Pt/MnO_x/SiO_2$ after an Oxidative or Reductive Pretreatment (in Arbitrary Units)

	A_{-NCO}	
Pretreatment	Sequence CO/NO[a]	Sequence NO/CO[a]
Reduction	14.4	8.2
Oxidation	7.5	4.3

[a] The sequence of addition of CO and NO was varied. CO/NO means that CO was adsorbed first, whereafter the temperature was raised to 300°C. After cooling to room temperature, NO was added. This sequence was reversed in the case of NO/CO. This means that only in the case of a reductive pretreatment and CO/NO sequence or in case of an oxidative pretreatment and NO/CO sequence, is the MnO_x of the catalyst severely reduced or fully reoxidized, respectively.

After an oxidative pretreatment with CO added first or after a reductive pretreatment with NO added first, the isocyanate band areas are almost equal. The value was lowest after an oxidative pretreatment and the sequence of addition NO/CO.

Since we may expect that the dissociation of NO on the platinum surface is inhibited by CO, NO must be dissociated by the partially reduced MnO_x. Contrary to $50CoO_x/SiO_2$, MnO_x/SiO_2 is able to form isocyanates after a reductive pretreatment. Spillover of CO_a from Pt to N_a on MnO_x, according to Model 2 (mentioned earlier in the section $Pt/50CoO_x/SiO_2$), is not necessary as it probably is on $Pt/CoO_x/SiO_2$. Model 2 is not necessary to explain the formation of –NCO on manganese oxide, but that does not mean that Model 2 can be excluded in the case of $Pt/MnO_x/SiO_2$. On a temperature rise the band area of –NCO increases with decreasing band area of Pt–CO (Fig. 8), which may be an indication of spillover of CO_a from Pt to N_a on MnO_x.

The area under the Pt–CO band changed also with the pretreatment. The area after an oxidative pretreatment is about twice as large as after a reductive pretreatment. It is known from the literature (34) that easily reducible metal oxides may migrate onto noble metals on reductive pretreatment. The noble metal is then partly decorated with partially reduced metal oxide, thereby influencing the adsorptive properties of the noble metal. Table 1 shows indeed that the Pt dispersion found with CO chemisorption is lowered by the addition of Mn. This partial covering of the Pt surface will result in retardation of some reactions or changes in the selectivity of certain reactions (34). Reoxidation restores the original adsorptive properties of the noble metal to a large extent, leaving only patches of reoxidized metal oxide on the noble metal surfaces.

From XRD it was found that on reduction MnO was formed. Imagine that MnO partly decorates Pt, leading to a decease in CO adsorption on Pt. There are more centers for NO dissociation on the partially reduced manganese oxide leading to more –NCO formation. Oxidation leads to a clean Pt surface and fewer dissociation centers on MnO_2, so a higher Pt–CO band area and a reduced –NCO band area will be found.

After an oxidative pretreatment the manganese oxide is oxidized to MnO_2, resulting in fewer sites for NO dissociation and the formation of –NCO bands. The addition of NO after a reductive pretreatment and the concomitant heating in 5 mbar NO to 300°C result in partial reoxidation of the manganese oxide. Probably part of the N_a formed on NO dissociation remains on the surface and may react with CO to isocyanate. After an oxidative pretreatment, addition of CO and concomitant heating to 300°C may result again in partially reduced MnO_x, with a reduction degree that is almost the same as after a reductive pretreatment and heating in an oxidizing NO atmosphere. There treatments may be similar to a mild reduction.

CONCLUSIONS

It was shown that the addition of metal oxides, such as cobalt and manganese oxide, to a standard Pt/SiO_2 catalyst did not change Pt particle size. For the higher cobalt-loaded $Pt/50CoO_x/SiO_2$ catalyst, a Pt–Co alloy phase could be identified after a reductive pretreatment.

The $50CoO_x/SiO_2$ did not form –NCO at the temperatures studied, while the formation of –NCO started at around 150°C over $Pt/CoO_x/SiO_2$ and $Pt/50CoO_x/SiO_2$ after a reductive pretreatment. It is most likely that CO_a adsorbed on Pt spilled over to N_a on the cobalt oxide.

The manganese oxide-containing catalysts showed a different behavior. Isocyanate formation started at around 250°C on MnO_x/SiO_2, while on $Pt/MnO_x/SiO_2$, –NCO was found above 150°C. The area under the –NCO band was measured, and the area after a reductive pretreatment was about three times larger than after an oxidative pretreatment. More NO dissociation centers are present on the $Pt/MnO_x/SiO_2$ catalyst after a reductive pretreatment than after oxidation.

It is beyond the scope of this paper to discuss in detail the role of CoO_x and MnO_x in the performance of the catalyst in CO oxidation and NO reduction. The present results suggest that Mn and Co are in the oxidic state under reaction conditions and that MnO_x and CoO_x are active components of the Pt-based catalysts in NO reduction and CO oxidation reactions.

ACKNOWLEDGMENTS

Funding for this project was provided through SON/STW (Project 349 1878). The Johnson Matthey Technology Centre (Reading, U.K.) is acknowledged for the loan of the Pt salts.

REFERENCES

1. Taylor, K. C., *in* "Automotive Catalytic Converters." Springer, Berlin, 1984.
2. Taylor, K. C., *Catal. Rev. Sci. Eng.* **35**, 457 (1993).
3. Kummer, J. T., *J. Phys. Chem.* **90**, 4747 (1986).
4. Mergler, Y. J., Chandoesing, R., and Nieuwenhuys, B. E., *Stud. Surf. Sci. Catal.* **96**, 163 (1995).
5. Mergler, Y. J., van Aalst, A., and Nieuwenhuys, B. E., *ACS Symp. Ser.* **587**, 196 (1995).
6. Mergler, Y. J., Van Aalst, A., Van Delft, J., and Nieuwenhuys, B. E., to be published.
7. Mergler, Y. J., Hoebink, J., and Nieuwenhuys, B. E., submitted for publication.
8. Mergler, Y. J., Van Aalst, A., Van Delft, J., and Nieuwenhuys, submitted for publication.
9. Davydov, A. A., *in* "IR Spectroscopy of Adsorbed Species on the Surface of Transition Metal Oxides," Chap. 4. Wiley, 1990.
10. Wielers, A. F. H., van der Grift, C. J. G., and Geus, J. W., *Appl. Catal.* **25**, 249 (1986).
11. De Jong, K. P., Meima, G. R., and Geus, J. W., *Appl. Surf. Sci.* **14**, 73 (1982).
12. Ponec, V., *Adv. Catal.* **32**, 149 (1983).
13. Geus, J. W., Dutch Patent Application 6, **705**, 259 (1967).
14. Geus, J. W., and van Leeuwen, P. W. N. M., *in* "Catalysis, an Integrated Approach to Homogeneous, Heterogeneous and Industrial Catalysts"

(J. A. Moulijn, P. W. N. M. van Leeuwen, and R. A. van Santen, Eds.), NIOK. Elsevier, Amsterdam, 1993.
15. Glaser, F., *Z. Anorg. Chem.* **36**, 25 (1903).
16. Guczi, L., Hoffer, T., Zsoldos, Z., Zyade, S., Maire, G., and Garin, F., *J. Phys. Chem.* **95**, 802 (1991).
17. Zsoldos, Z., and Guczi, L., *J. Phys. Chem.* **96**, 9393 (1992).
18. Potoczna-Petru, D., and Kepiński, L., *Catal. Lett.* **9**, 355 (1991).
19. Alikina, G. M., Davydov, A. A., and Sazonova, I. S., *Kinet. Katal.* **27**, 875 (1986).
20. Busca, G., Guidetti, R., and Lorenzelli, V., *J. Chem. Soc. Faraday Trans.* **86**, 989 (1990).
21. Niiyama, H., and Echigoya, E., *J. Catal.* **38**, 238 (1975).
22. Ishihara, T., Eguchi, K., and Arai, H., *Chem. Lett.* 1695 (1986).
23. Ansorge, J., and Förster, H., *Z. Phys. Chem. N.F.* **118**, 113 (1979).
24. Choi, J.-G., Rhee, H.-K., and Moon, S. H., *Kor. J. Chem. Eng.* **1**, 159 (1984).
25. Gopalakrishnan, R., and Viswanathan, B., *J. Colloid Interface Sci.* **102**, 370 (1984).
26. Toolenaar, F. J. C. M., Stoop, F., and Ponec, V., *J. Catal.* **82**, 1 (1983).
27. Bastein, A. G. T. M., Toolenaar, F. J. C. M., and Ponec, V., *J. Catal.* **90**, 88 (1984).
28. Dees, M. J., Shido, T., Iwasawa, Y., and Ponec, V., *J. Catal.* **124**, 530 (1990).
29. Yao, H. C., and Shelef, M., *J. Phys. Chem.* **78**, 2490 (1974).
30. Solymosi, F., Völgyesi, L., and Sárkány, J., *J. Catal.* **54**, 336 (1978).
31. Hecker, W. C., and Bell, A. T., *J. Catal.* **85**, 389 (1984).
32. Anderson, J. A., and Rochester, C. H., *J. Chem. Soc. Faraday Trans.* **86**, 3809 (1990).
33. Anderson, J. A., *J. Chem. Soc. Faraday Trans.* **88**, 1197 (1992).
34. Sanchez, M. G., and Gazquez, J. L., *J. Catal.* **104**, 120 (1987), and references therein.